UC Davis
UC Davis Previously Published Works

Title

Interrelation between Structure – Magnetic Properties in La0.5Sr0.5CoO3

Permalink

Journal

ISSN

Authors

Biegalski, Michael D
Takamura, Yayoi
Mehta, Apurva
et al.

Publication Date

DOI

Peer reviewed

www.MaterialsViews.com

ADVANCED
MATERIALS
INTERFACES
www.advmatinterfaces.de

COMMUNICATION

Interrelation between Structure – Magnetic Properties in La$_{0.5}$Sr$_{0.5}$CoO$_3$

Michael. D. Biegalski,* Yayoi Takamura, Apurva Mehta, Zhang Gai, Sergei V. Kalinin, Haile Ambaye, Valieria Lauter, Dillon Fong, Sokrates T. Pantelides, Young. M. Kim, Jun. He, Albina Borisevich, Wolter Siemons, and Hans M. Christen

Due to the strong interaction amongst the charge, spin, orbital, and lattice degrees of freedom, the perovskite oxides (ABO$_3$) possess a wide range of technologically relevant properties such as magnetism, ferroelectricity, and superconductivity.[1] While the properties of a material may be well-known in the bulk, its incorporation into a device structure as a thin film or superlattice can result in a rich and unanticipated array of new physical phenomena.[2,3] Key drivers of this change include the epitaxial strain imposed from the underlying substrate, the structural and chemical properties of the interfaces, as well as induced electronic and/or magnetic interactions. On one hand, these strong correlations between the atomic structure of thin films and their chemical and electronic properties pose a severe challenge to our current understanding of the origin of properties. On the other hand, a progressively better understanding of these correlations can lead to materials designed at the atomic

Dr. M. D. Biegalski, Dr. Z. Gai, Dr. S. V. Kalinin,
Dr. H. M. Christen
Center for Nanophase Materials Science
Oak Ridge National Laboratory
Oak Ridge, TN 37830, USA
E-mail: biegalskim@ornl.gov
Prof. Y. Takamura
Dept. of Chemical Engineering and Materials Science
University of California
Davis, CA 95616, USA
Dr. A. Mehta
Stanford Synchrotron Radiation Lightsource
Menlo Park, CA 94025, USA
Dr. H. Ambaye, Dr. V. Lauter
Neutron Scattering Sciences Division
Oak Ridge National Laboratory
Oak Ridge, TN 37830, USA
Dr. D. Fong
Materials Scientist, Materials Science Division
Argonne National Laboratory
Argonne, IL 60439, USA
Prof. S. T. Pantelides
Dept. of Physics and Astronomy
Vanderbilt University
Nashville, TN 37235, USA
Dr. Y. M. Kim
Korea Basic Science Institute
Daejeon 305-806, Korea
Dr. J. He, Dr. Y. M. Kim, Dr. W. Siemons, Dr. A. Borisevich
Materials Science and Technology
Division, Oak Ridge National
Laboratory, Oak, Ridge, TN, 37830, USA

scale and tailored to have desired properties. Modern synthesis techniques, for instance, can exploit this deeper understanding of structure – property relationships and fabricate epitaxial superlattices composed of alternating layers, each with their own functional property and the complete stack operating as a highly complex and self-contained device.[4,5]

The ideal perovskite structure has cubic symmetry characterized by BO$_6$ octahedra with equal B-O bond angles/distances in all directions. However, differences in the ionic radii of the A and B atoms lead to tilts and rotations of the octahedra and lowering of structural symmetry. Glazer[6] devised a notation to describe these tilts along the three principle crystallographic directions and tabulated the families of half-order peaks associated with various lowered structural symmetries. In epitaxial films, the lattice mismatch between the film and the substrate results in differing in-plane vs. out-of-plane bond angles/distances; and/or to a change in the pattern of BO$_6$ tilts/rotations. These structural distortions occur commonly in perovskites and while several theoretical studies have highlighted their impact on the functional properties,[7–10] few detailed experimental studies have been performed to fully understand and explore these structure-property relationships.[11]–[13]

Strontium doped lanthanum cobaltite La$_{1-x}$Sr$_x$CO$_3$ (LSCO) was chosen as a model system for the current study for two reasons. LSCO shows a rich magnetic phase diagram, ranging from a spin glass with $x < 0.18$ to strong ferromagnetic behavior at $x > 0.3$.[14] In addition, CoO$_6$ octahedra are more likely to rotate and maintain the octahedral tilt pattern that is imposed at the interface because the octahedra do not show strong Jahn Teller distortions like La$_{1-x}$Sr$_x$MnO$_3$ (LSMO).[15] This rigidity of the octahedra is necessary for the effects of the long range properties to be examined with bulk techniques and differs greatly from that found in other similar perovskites such as LSMO or BiFeO$_3$ where the tilts have been found to return to bulk tilt patterns within a few unit cells of the interface, presumably requiring the distortion of octahedra.[8,16]–[18] This robustness of the octahedra simplify the exploration of structure – property relationships by limiting the number of possible structure distortions to either overall lattice distortion, octahedral tilts or a combination of the two within this system.

We grew epitaxial thin films (thickness = 100 Å) of (La$_{0.5}$Sr$_{0.5}$)CoO$_3$ on two different substrates, (001)-oriented La$_{0.30}$Sr$_{0.70}$Al$_{0.65}$Ta$_{0.35}$O$_3$ (LSAT) and (101)-oriented NdGaO$_3$ (NGO), with nearly identical in-plane lattice parameters but different structures. LSAT has a cubic structure with lattice parameter of 3.870 Å and no tilting of the BO$_6$ octahedra (**Figure 1**a), i.e. an $a^0a^0a^0$ tilt structure in Glazer's notation.[19] In contrast,

Figure 1. a) Schematic showing the impact of epitaxy on the octahedral tilts in LSCO. The atomic structures of the bulk LSAT, NGO, and LSCO are shown in the top half of the figure and the expected octahedral tilt structure of LSCO is shown on LSAT and NGO. The RSMs around the 303_{pc} peaks are shown for 100 Å thick LSCO on LSAT (b) and NGO (c) and indicate the differences in symmetries between the tetragonal-like LSCO on LSAT to the monoclinic-type structure on NGO. Horizontal lines indicate the out-of-plane lattice spacing for the different axes. The scans through the half-integer peaks show strong peaks for films on NGO (d,f) while only show peaks for the substrate for films on LSAT (e, g).

NGO is orthorhombic (space group: Pbnm) with the $a^-b^+a^-$ tilt symmetry, and lattice parameters of $a = 5.44$ Å, $b = 7.71$ Å, and $c = 5.50$ Å. Using a pseudocubic representation, (101)-oriented NGO substrate can be redefined by a $(020) \parallel (010)_{pc}$ and $[101] \parallel [001]_{pc}$ transformation to yield a rectangular in-plane growth net of 3.855 Å by 3.863 Å. The average in-plane lattice parameters for the two substrates, LSAT and NGO, thus, differ by less than 0.3%, however, because they have different oxygen octahedral tilt (OOT) symmetry, the in-plane growth net for one is square whereas it is rectangular for the other. Coherently grown LSCO films on these two substrates will allow separation of the effects of OOT from the effects of strain induced by gross epitaxial mismatch.[8,22] The effect of these different substrates has been recently explored for the magnetic properties of ultrathin $La_{0.67}Sr_{0.33}MnO_3$. This study found that octahedral rotations resulting from interfacial coupling can directly affect

www.MaterialsViews.com

ADVANCED
MATERIALS
INTERFACES
www.advmatinterfaces.de

COMMUNICATION

the magnetization and transport properties of the films. Our results show similar effect of the control of the octahedral tilting within the thin film through the substrate, however unlike this previous study, within the LSCO system, the deviation from bulk tilting it is preserved throughout the entirety of the 10 nm thick film as evidenced by X-ray diffraction (XRD) and transmission electron microscopy results. In 10 nm thick LSCO films, we find that the LSCO octahedral tilts are slightly suppressed under tensile strain when grown on NGO, however the tilts are almost entirely suppressed when grown on LSAT. This difference is also reflected in the magnetic properties where the magnetic moment of LSCO is reduced for films grown on LSAT as compared to NGO. The differences in magnetism are shown through density functional theory (DFT) modeling to be accountable by the impact of the octahedral tilting differences on the electronic structure of the material.

Detailed structural characterization performed by XRD showed that the symmetry of the LSCO films is strongly dependent on the substrate (Figure 1). Based on the analysis of several XRD peaks, (lattice parameters summarized in Table S1) and combined with the reciprocal space maps (RSM) around the 303_{pc} type peaks (Figure 1b and 1c) illustrate that the symmetry of the LSCO films is strongly dependent on the substrate. The LSCO film grown on LSAT is tetragonal with all 4 LSCO peaks at the same position while LSCO on NGO has symmetry no higher than orthorhombic with different positions for the LSCO 303_{pc} type peaks. Furthermore, the RSM and lattice constants indicate that the films are fully commensurate with the substrate. It should be noted that the $00L_{pc}$ rods do not show any trace of the brownmillerite structure reported for some LSCO thin films.[20]

As shown extensively over the last 40 years, deviation of a perovskite structure with cubic symmetry frequently results in doubling of the unit cell. Glazer and many other subsequent researchers demonstrated that the symmetry of the perovskite structure can be determined from the intensities of the superlattices peaks occurring at half integer positions in a pseudocubic reciprocal lattice.[19] No half integer peaks or even shoulders from the LSCO film were found on LSAT from the several half order peaks investigated, with the exception of a few broad peaks also found for a bare LSAT substrate (see Figure 1d–1g.). These measurements indicate that LSCO films, when grown fully commensurate on cubic substrates such as LSAT, crystallize in tetragonal symmetry with an $a^0a^0a^0$ OOT system in Glazer notation. (Extremely small distortions (<1°) from the tetragonal symmetry would be beyond the resolution of this technique.) On the other hand, several relatively strong half integer peaks with instrument limited narrow in-plane (H and K) widths were found for the LSCO film on NGO. These extremely narrow peak widths of the half order peaks indicate that the octahedral tilting of the LSCO in this film is coherent throughout the thickness of the films. These are located adjacent to the much stronger half integer peaks from the substrate (see Figure 1d–1g). A systematic survey of the observed peaks indicated

that only odd half integer peaks (i.e., $(2m+1/2)H$, $(2n+1/2)K$, $(2o+1/2)L$) in the pseudocubic lattice) exist, suggesting that the film has crystallized in either an triclinic lattice with $a^-b^-c^-$ tilts or a monoclinic lattice with $a^0b^-c^-$ OOT in Glazer notation.[19] Our results cannot rule out a triclinic structure but it is unlikely given that the films are completely coherent with the orthorhombic substrate. The possibility of oxygen vacancy ordering affecting the half order reflections was investigated with no evidence of any half order peaks on the 00L rod in Figure S1 and no peaks present at the 111 or 333 half order positions. Furthermore, we were able to quantify OOT angles around the three crystallographic axes (α, β and γ) by fitting the relative intensities of the half integer peaks using the method described by May et al.[13] The tilt angles were found to be $\alpha =$ 0°, $\beta = 2.4°$, and $\gamma = 6.3°$, with an estimated error of ~1° (Details are summarized supplemental Table S2). Most of the error in this estimation came from the imprecision of fitting a lower-intensity film peak in close proximity to a much stronger substrate peak. These tilt angles also do not completely explain the deviation from the bulk lattice parameters indicating the epitaxial strain is not accommodated by changes in the octahedral tilts, rather the majority of the strain is accommodated through bond length changes, which also requires slight distortions of the octahedra as previously calculated for similar systems.[9] Furthermore, this tilt pattern differs from that of the substrate ($a^-b^+a^-$) and the bulk material ($a^-a^-a^-$), and is unrelated to either by group-subgroup relationship, suggesting that the transition between them must be discontinuous.[21] Therefore, these results indicate that the long range symmetry of the epitaxial film is not strongly dependent on the tilt symmetry of the substrate, rather mostly a response that attempts to minimize long-range strain from the anisotropy of the rectangular in-plane growth net. These structural differences are expected to lead to different magnetic properties as discussed in the following section.

AC susceptibility measurements (**Figure 2**a) show that the Curie temperature, T_C is ~190 K, regardless of the substrate. The Curie temperature in LSCO is known to be highly sensitive to composition (La:Sr ratio and oxygen stoichiometry), therefore this agreement confirms the similarity in compositions of the LSCO films grown on both substrates.[22] The large paramagnetic moment of the Nd ions does not allow a direct measurement of the DC magnetization of films on NGO substrates.
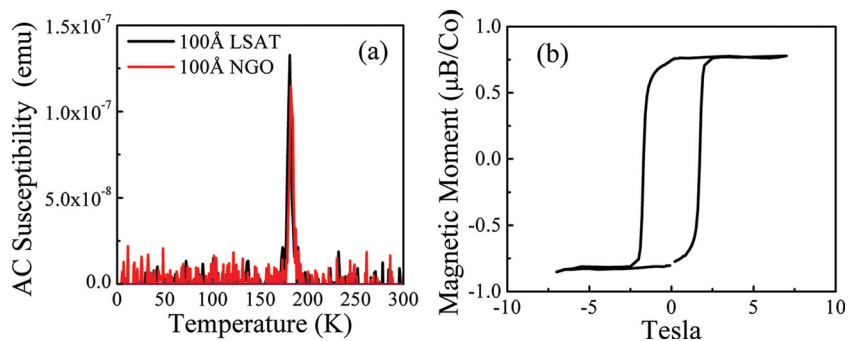
Figure 2. The AC magnetization show that the T_c for the 100 Å thick films are near 190K for films grown on LSAT and NGO. The SQUID M-H loop for LSCO films grown on LSAT shows a saturation moment of 0.78 µB/Co .

**ADVANCED
MATERIALS
INTERFACES**

www.advmatinterfaces.de

*Materials
Views*

www.MaterialsViews.com
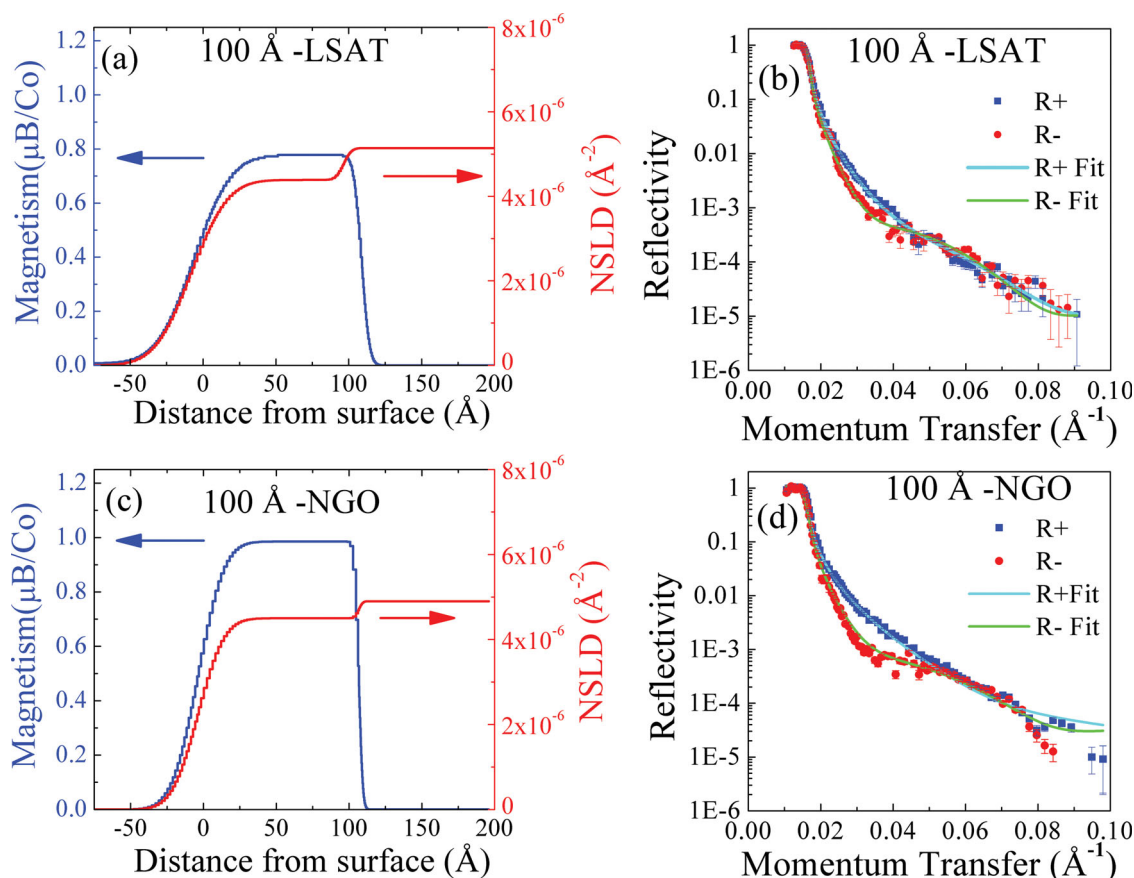
Figure 3. PNR data taken at 10K show that the resulting magnetism in the LSCO films is higher for films grown on NGO as compared to LSAT. The depth profiles of the magnetism and scattering length density (2a and 2c) show that fitting resutls in similar depth profiles but different magentizations. The two polarization states of the incident neutrons are marked with blue squares and red circles for +/− polarizations respectively. Error bars are marked on the data. The fits from models (2b and 2d) are overlaid on the data and accurately describe the data with a simple model of a single layer 100 Å thick film with surface and interface roughness.

Therefore, polarized neutron reflectometry (PNR) performed at beamline 4a at the Spallation Neutron Source was used to determine the magnetic moment of these films. PNR provides depth-resolved magnetization information and is insensitive to the paramagnetic moment of the substrate.[23] The LSCO films were field cooled down to 10 K and measurements were made with neutrons with alternating polarization states, +/− polarized, to ascertain the magnetic properties of the films. For all films, the PNR data were well fit with a model consisting of a substrate layer, single film layer (i.e. uniform magnetization across the entire film thickness), and a roughness layer at the interface, as has been previously performed for similar films.[24] The film grown on NGO shows a higher magnetization of 0.98 μ_B/Co than the film grown on LSAT (0.77 μ_B/Co), [1]however both films show much weaker magnetization than bulk LSCO (1.92 μ_B/Co).[25] This reduced moment is in agreement with similar studies of strained LSCO films of this thickness.[26] The resulting magnetization from the PNR experiments is summarized in **Figure 3** along with the experimental fitting and data. The magnetization of the LSCO film grown on LSAT was also

confirmed using SQUID magnetometry (Figure 2b). The presence of point defects such as antisite defects and oxygen vacancies which may affect the magnetic properties cannot be ruled out, however, EELS analysis shows that the films have equal Co valence states (Co L_2/L_3 ratios) indicating that the stoichiometry and defect states of the samples are similar.[20] Thus, the differences in magnetic properties between these two samples are attributed to the changes in the structure of the films.

From a simple crystal-field splitting picture for LaCoO$_3$ (LCO) that a deviation of the Co-O-Co bond angle from 180° caused by OOT is predicted to suppress T_C.[27] However, the T_C of the LSCO films studied here remained unchanged regardless of whether the Co-O-Co bond angles deviated from 180° as in the case of the film grown on NGO, or had no octahedral distortions (film grown on LSAT). This result indicates that the magnetization of LSCO is driven by a mechanism that differs from that in LCO.

In order to better understand the impact of structural distortions of the epitaxial LSCO films on electronic structure, and specifically magnetism, DFT calculations were performed for a several tilt structures and strain states that were observed in the XRD measurements. The modeled tilt systems were refined from the best fit to the half integer XRD data assuming either an $a^0b^-c^-$, $a^-b^0c^-$ or $a^-b^-c^-$ tilt system. To address the

[1]The measured magnetism has an error of ~0.03 μ_B/Co with the fitting method.

www.MaterialsViews.com

ADVANCED
MATERIALS
INTERFACES
www.advmatinterfaces.de

COMMUNICATION

LSCO films grown on LSAT, an un-tilted $a^0a^0a^0$ system was also modeled. The stability of each of the structures relative to each other, as well as their electronic structures (and hence magnetic properties) was calculated. For each of these imposed tilt systems three different strain states were modeled: first an unstrained – fully relaxed – lattice, second a lattice with equal in-plane strain of 1% (similar to films on LSAT), and third a lattice with an asymmetric in-plane strain on average of 1% (similar to films on NGO). All these strain states had an imposed tilt symmetry that was not allowed to relax during the modeling. A summary of the DFT results is shown in **Table 1**. Though the quantitative predictions of the DFT calculations are not in agreement with our measurements, in that they do not fully account for the reduced dimensionality or proximity to the substrate, the relative changes predicted are in good qualitative agreement and lead to several important insights into the relationship between ionic and electronic lattices, and the relationship between magnetism and structural distortions in LSCO.

Three salient structural implications clearly emerge from the DFT calculations. First, for all cases considered, epitaxial strain increases the free energy. Second, for both unstrained and strained systems, the lowest energy structure was found for a film with the $a^0b^-c^-$ tilts, i.e. the symmetry observed for the LSCO film on NGO. Finally, the film with 1% strained and un-tilted structure on a cubic substrate, i.e. the symmetry observed for a film on LSAT, was the structure with the highest energy, indicating that this is the least stable structure. This suggests that the presences of cubic LSAT substrate exerts a strong stabilizing force on the LSCO to enable the un-tilted LSCO film structure to be present. Furthermore, the higher energy of the LSCO in this state suggests that under tensile strain, this would be very difficult system to stabilize in agreement with our experience with thicker film LSCO films on LSAT.

The DFT calculations also show that the structural distortions strongly impact the electronic structure in that any structural distortion, be it epitaxial strain or OOT, away from cubic symmetry further lowers the degeneracy of the Co d orbitals from the well-established splitting in octahedral ligand field (into 3-fold degenerate t_{2g} and 2-fold degenerate e_g states). Though the distortions break the degeneracy of both t_{2g} and e_g states, splitting of the t_{2g} states has the most impact on magnetizations because it, tends to move the spin-up electrons from the higher states through a spin-flip transition to pair with the spin-up electron in the lowest t_{2g} state, thereby decreasing the number of unpaired electrons and hence the magnetization. Density of states near the Fermi level for the four structures most relevant to this study, namely, a cubic structure, a structure with 1% epitaxial strain but no tilts, a structure with $a^0b^-c^-$ tilts but no strain, and a structure with both epitaxial strain and OOT, and a schematic representation of the filling of d orbitals are shown in **Figure 4**.

Four main conclusions concerning the effects of structural distortion on the electronic structure and magnetization also emerge from the DFT calculations. First (results not shown), the asymmetry of the in-plane growth net has minimal impact on the magnetization, i.e., going from square ($a = b$) net, for films on a substrate such LSAT, to a rectangular ($a<b$) net, for a film on a substrate such as NGO, by itself is not sufficient

Table 1. Calculated free energy and magnetization per unit cell for LSCO with different tilt structures and three strain states: relaxed, 1% strain with equal in-plane lattice constants, and with unequal in-plane lattice constants. These results show that for an unstrained unit cell, the decrease of the Co-O-Co bond angle decreases the magnetization, as observed in bulk. However, for strained LSCO films, the same changes in tilts have a different effect on the magnetism, and the $a^0b^-c^-$ tilt pattern shows the highest magnetism with a 1% strain. Note: the energies were normalized to the lowest energy state calculated, the $a^0b^-c^-$ tilt structure without any strain.

	No strain Relaxed	1% Strain $a = b$	1% Strain $a < b$
No tilts $a^0b^0c^0$	0.33 eV	0.55 eV	0.50 eV
	2.07 μB	1.80 μB	1.80 μB
$a^0b^-c^-$ tilts $\alpha = 0$ $\beta = 2.4$ $\gamma = 6.3$	0 eV	0.15 eV	0.11eV
	1.90 μB	1.76 μB	1.94 μB
$a^-b^0c^-$ tilts $\alpha = 8.8$ $\beta = 0$ $\gamma = 5.2$	0.08 eV	0.25 eV	0.19 eV
	1.89 μB	1.82 μB	1.81 μB
$a^-b^-c^-$ tilts $\alpha = 5.6$ $\beta = 3.4$ $\gamma = 8.4$	0.18 eV	0.32 eV	0.16 eV
	1.75 μB	1.83 μB	1.78 μB

to alter the magnetization. Second, while epitaxial strain and $a^0b^-c^-$ OOT distortion independently lower magnetization, interestingly, the combination of the two, i.e., in a structure similar to LSCO on NGO, partially restores the degeneracy between two of the three t_{2g} states, thereby increasing the number of unpaired spins and restoring some of the lost magnetization. Third, the DFT calculations, in good qualitative agreement with observations, predict the $a^0b^-c^-$ tilted LSCO film to have the highest magnetization of all the strained epitaxial LSCO films considered, and an epitaxially strained but un-tilted film, not dissimilar to a film grown on LSAT, to have the lowest magnetization. Finally, the other calculated tilt systems do not show significant increase in magnetization. Taken together, all these points suggest that a fine balance exists between lattice distortion through overall strain and octahedral tilts, which leads to the most degenerate d band electronic structure and the highest magnetization for the system possible.

In summary, the interplay between the structural parameters (octahedral tilts and strain) and the electronic structure and resulting magnetization in LSCO illustrates the tradeoffs which exist between the competing ordering parameters and that can result in unexpected correlations between properties in perovskite materials. Furthermore, this work demonstrates that asymmetric epitaxial strain controls not only the strain state through the film/substrate lattice mismatch but also the OOT symmetry through the symmetry of the substrate, and therefore offers a mechanism to control the properties in oxide thin films. This study highlights the strong interactions as well as the delicate and predictively difficult balance among competing drivers, such as octahedral tilting, overall strain, and electronic structure that determine truly quantum phenomena, such as magnetism or superconductivity. The need for a quantitatively accurate understanding of relationships between structure and quantum properties in complex materials, therefore, will stimulate further combined experimental and theoretical investigations as discussed here.
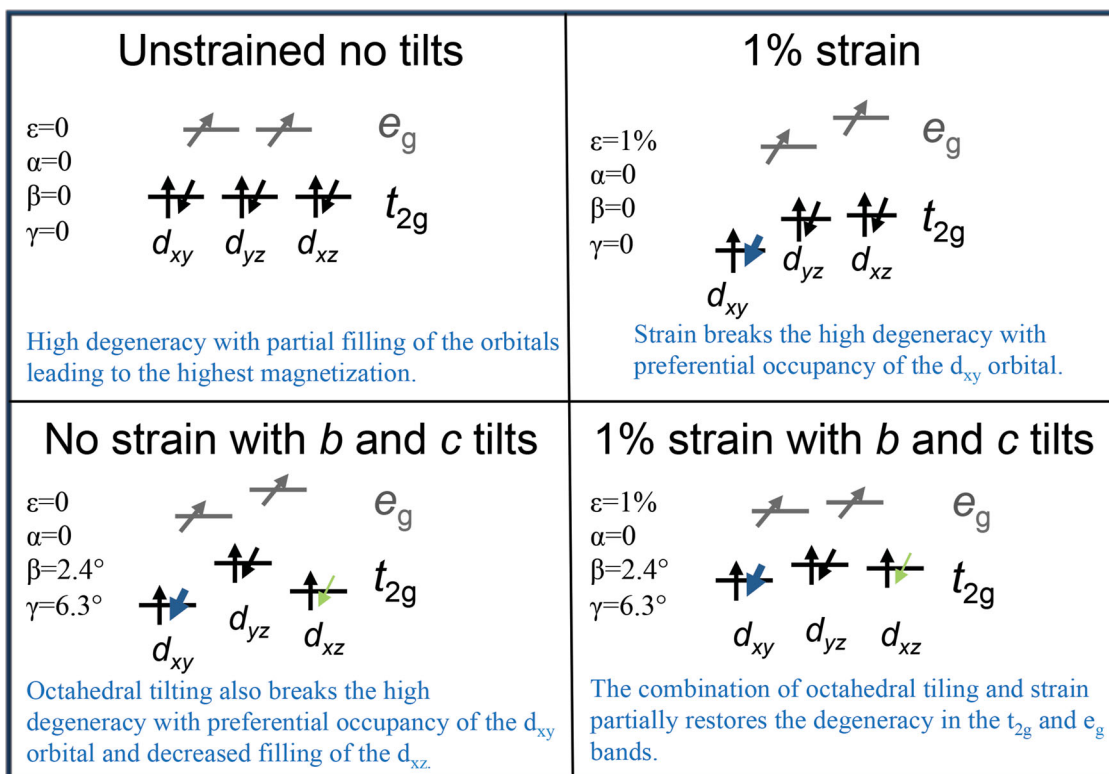
Figure 4. The effect of octahedral tilting and strain on the orbital filling and degeneracy of the t_{2g} and e_g states. Tilted arrows indicate that the state is partially occupied, green/blue arrows indicating a less/more occupied state. In the unstrained pseudocubic state, the orbitals are all highly degenerate, leading to strong magnetism in LSCO. Once tilts are added, the degeneracy of the orbitals decreases, causing the orbital filling to change, as denoted by the larger blue arrows for increased filling in the t_{2g} states and thinner green arrows for decreased filling in the e_g states. However, for the case of an asymmetrically strained LSCO with the $a^0b^-c^-$ tilt structure, the degeneracy is partially restored, inducing a configuration closer to the unstrained state.

Experimental Section

The LSCO films were grown on LSAT and NGO substrates using pulsed laser deposition PLD successively under identical growth conditions and slowly cooled to room temperature in 200 Torr of pure oxygen to ensure fully oxidizing the LSCO. The symmetries and lattice constants of the LSCO thin films were determined using a PANalytical MRD with Hybrid monochrometer and triple-axis analyzer crystal. Measurements of half integer peaks were performed at 15 KeV on beam line 7–2 at the Stanford Synchrotron Radiation Lightsource. Magnetic properties of the films were determined using a Quantum Design MPMS and Polarized Neutron Reflectometry was performed at beam line 4a at the Spallation Neutron Source at 10 K, under a field of 1.1 Tesla. DFT calculation of the electronic structure and magnetic properties were modeled within the framework of the projector-augmented-wave method implemented in the Vienna ab initio Simulation Package (VASP).[28,29] The calculations were based on a $2\times2\times2$ supercell of 40 atoms, which could fully express the octahedral tilt structure. The spin-polarized generalized-gradient approximations were applied and the magnetic states are relaxed in collinear configurations. In order to analyze the strained LSCO films that were coherent to the NGO and LSAT substrates, the lattice parameters of NGO were calculated and the in-plane LSCO lattice parameters were then strained to these DFT determined NGO lattice parameters.

Supporting Information

Supporting Information is available from the Wiley Online Library or from the author.

[1] E. Dagotto, *Science* **2005**, *309*, 257–262.
[2] J. Mannhart, D. G. Schlom, *Science* **2010**, *327*, 1607–1611.
[3] K. J. Choi, M. D. Biegalski, Y. L Li, A. Sharan, J. Schubert, R. Uecker, P. Reiche, Y. B. Chen, X. Q. Pan, V. Gopalan, L. Q. Chen, D. G. Schlom, C. B. Eom, *Science* **2004**, *306*, 1005–1009.
[4] D. G. Schlom, L.-Q. Chen, X. Q. Pan, A. Schmehl, M. A. Zurbuchen, *J. Am. Ceram. Soc.* **2008**, *91*, 2429–2454.
[5] S. A. Chambers, *Adv. Mater.* **2010**, *22*, 219–248.
[6] A. M. Glazer, *Acta Crystallogr., Sect. B: Struct. Crystallogr. Cryst. Chem.* **1972**, *28*, 3384–3392.
[7] J. M. Rondinelli, N. A. Spaldin, *Phys. Rev. B* **2009**, *79*, 054409.
[8] E. J. Moon, P. V. Balachandran, B. J. Kirby, D. J. Keavney, R. J. Sichel-Tissot, C. M. Schlepütz, E. Karapetrova, X. M. Cheng, J. M. Rondinelli, S. J. May *Nano Lett.* DOI 10.1021/nl500235.
[9] J. M. Rondinelli, N. A. Spaldin, *Phys. Rev. B* **2010**, *81*, 085109.

[10] K. Gupta, P. Mahadevan, *Phys. Rev. B* **2009**, *79*, 020406(R).

[11] A. Vailionis, H. Boschker, W. Siemons, E. P. Houwman, D. H. A. Blank, G. Rijnders, G. Koster, *Phys. Rev. B* **2011**, *83*, 064101.

[12] A. Borisevich, H. J. Chang, M. Huijben, M. P. Oxley, S. Okamoto, M. K. Niranjan, J. D. Burton, E. Y. Tsymbal, Y. H. Chu, P. Yu, R. Ramesh, S. V. Kalinin, S. J. Pennycook, *Phys. Rev. Lett.* **2010**, *105*, 087204.

[13] S. J. May, J.-W. Kim, J. M. Rondinelli, E. Karapetrova, N. A. Spaldin, A. Bhattacharya, P. J. Ryan, *Phys. Rev. B* **2010**, *82*, 014110.

[14] P. M. Raccah, J. B. Goodenough, *J. Appl. Phys.* **1968**, *39*, 1209–1210.

[15] N. Sundaram, Y. Jiang, I. E. Anderson, D. P. Belanger, C. H. Booth, F. Bridges, J. Mitchel, Th., Proffen , H. Zheng, *Phys. Rev. Lett* **2009**, *102*, 026401.

[16] R. Aso, A. Kan, Y. Shimakawa, H. Kurata, *Sci. Rep.* **2013**, *3*, 2214.

[17] A. Y. Borisevich, H. J. Chang, M. Huijben, M. P. Oxley, S. Okamoto, M. K. Niranjan, J. D. Burton, E. Y. Tsymbal, Y. H. Chu, P. Yu, R. Ramesh, S. V. Kalinin, S. J. Pennycook, *Phys. Rev. Lett.* **2010**, *105*, 087204.

[18] J. He, A. Borisevich, S. V. Kalinin, S. J. Pennycook, *Phys. Rev. Lett.* **2010**, *105*, 227203.

[19] A. M. Glazer, *Acta Cryst.* **1975**, *A31*, 756–762.

[20] Y.-M. Kim, J. He, M. D. Biegalski, H. Ambaye, V. Lauter, H. M. Christen, S. T. Pantelides, S. J. Pennycook, S. V. Kalinin, A. Y. Borisevich, *Nat. Mater.* **2012**, *11*, 888–894.

[21] C. J. Howard, H. T. Stokes, *Acta Cryst.* **2005**, *A61*, 93–111.

[22] C. K. Xie, J. I. Budnick, W. A. Hines, B. O. Wells, J. C. Woicik, *Appl. Phys. Lett.* **2008**, *93*, 182507.

[23] J. F. Anknera, G. P. Felcher, *J. Magnet. Magnet. Mater.* **1999**, *200*, 741.

[24] M. A. Torija, M. Sharma, M. R. Fitzsimmons, M. Varela, C. Leighton *J. Appl. Phys.* **2008**, *104*, 023901.

[25] J. Wu, J. W. Lynn, C. J. Glinka, J. Burley, H. Zheng, J. F. Mitchell, C. Leighton, *Phys. Rev. Lett.* **2005**, *94*, 037201.

[26] C. Xie, J. I. Budnick, B. O. Wells, J. C. Woicik, *Appl. Phys. Lett.* **2007**, *91*, 172509.

[27] D. Fuchs, E. Arac, C. Pinta, S. Schuppler, R. Schneider, H. v. Löhneysen, *Phys. Rev. B* **2008**, *77*, 014434.

[28] W. Kohn, L. J. Sham, *Phys. Rev.* **1965**, *140*, A1133.

[29] G. Kresse, J. Furthmüller, *Phys. Rev. B* **1996**, *54*, 11169.